

## Supplementary Information

### **Rational design of polyaromatic ionomers for alkaline membrane fuel cells with > 1 W cm<sup>-2</sup> power density**

Sandip Maurya,<sup>†a</sup> Sangtaik Noh,<sup>†b</sup> Ivana Matanovic,<sup>†cd</sup> Eun Joo Park,<sup>a</sup> Claudia Narvaez Villarrubia,<sup>a</sup> Ulises Martinez,<sup>a</sup> Junyoung Han,<sup>b</sup> Chulsung Bae,<sup>\*b</sup> and Yu Seung Kim<sup>\*a</sup>

a. MPA-11: Materials Synthesis & Integrated Devices, Los Alamos National Laboratory, Los Alamos, New Mexico 87545, USA

b. Department of Chemistry and Chemical Biology, Rensselaer Polytechnic Institute, Troy, New York 12180, USA

c. Department of Chemical and Biological Engineering, Center for Micro-Engineered Materials (CMEM), The University of New Mexico, Albuquerque, New Mexico 87231, USA

d. Theoretical Division, Los Alamos National Laboratory, Los Alamos 87545, USA

<sup>†</sup> Equal Contributors

This PDF file includes:

Experimental Procedure

Table S1

Figs. S1 to S10

References 1-17

## Experimental Procedure

### Density Functional Theory Calculations

The electronic structure calculations were performed using generalized gradient approximation (GGA) to density functional theory (DFT) with vdW-DF functional as proposed by Dion et al.<sup>1-3</sup> and projector augmented-wave pseudopotentials<sup>4,5</sup> using the Vienna Ab initio Software Package (VASP)<sup>6-9</sup>. Extended Pt(111) and Pt<sub>1</sub>Ru<sub>1</sub> (111) surfaces were modelled using supercells with the dimensions of 16.80 Å × 16.80 Å and 16.48 Å × 16.48 Å, respectively. These correspond to the unit cells of the size  $(3a\sqrt{2} \times 3b\sqrt{2})R\gamma$  where  $a$ ,  $b$ , and  $\gamma$  are the cell parameters determined from the bulk calculations. Both surfaces were modelled using three layers of metal atoms and a vacuum region of 20 Å, resulting in a unit cell with 108 metal atoms. To create the effect of the bulk, only the two top layers were allowed to relax until the convergence in the energy of 0.01 meV was achieved. The electronic energies were calculated using 4×4×1 k-point Monkhorst-Pack<sup>10</sup> mesh and Methfessel-Paxton smearing<sup>11</sup> of order 2 and with sigma set to 0.2. In all the cases, plane-wave basis cutoff was set to 400 eV. Adsorption energies were calculated using the following formula:

$$\Delta E_{\text{ad}} = E_{\text{surface+ad}} - [E_{\text{surface}} + E_{\text{ad}}]$$

where  $E_{\text{surface+ad}}$  is the energy of biphenyl and 9,9-dimethyl fluorene adsorbed on the Pt(111) or PtRu(111) surface,  $E_{\text{surface}}$  is the energy of the clean surface, and  $E_{\text{ad}}$  is the energy of biphenyl or 9,9-dimethyl fluorene in the gas phase. Several adsorption sites<sup>12,13</sup> and orientations of biphenyl and 9,9-dimethyl fluorene relative to the surface were tested, but in each case, the orientation in which the adsorbed molecules are parallel to the surface resulted in the highest adsorption energies. In the case of biphenyl, three conformations were tested with the torsion angles of 0°, 44°, and 90° between the phenyl rings. The 0° conformation in which both of the phenyl rings are adsorbed parallel to the surface has the highest adsorption energy and represent the most stable conformation of biphenyl when interacting with the surface of the catalyst (Figure S1).

### Materials

All reagents and solvents were used from commercial sources and used without further purification. <sup>1</sup>H NMR spectra were obtained with a 500MHz Agilent NMR spectrometer. 9,9-Bis(6-bromohexyl)fluorene was synthesized in the one-step reaction, following the reported procedures.<sup>14,15</sup>

### Synthesis of FLN precursor (FLBr-xx)

Typical acid-catalysed polymerization was conducted at 0 °C under nitrogen atmosphere. To a solution of 6 mmol of each of three monomers (molar ratio of 9,9-bis(6-bromohexyl)fluorene:9,9-dimethylfluorene:1,1,1-trifluoroacetone = m:n:1.2(m+n)) in 6 mL dry dichloromethane, triflic acid (4 mL) was added dropwise while stirring vigorously. When the viscosity of the solution was dramatically increased, the reaction mixture was poured into methanol with stirring to obtain crude polymer precipitate. The collected crude polymer was dissolved in THF and then re-precipitated in methanol for purification.

### Synthesis of FLN

Quarterization was conducted at ambient condition. To a THF solution of FLBr2-xx (xx = 30, 40, and 55), trimethylamine (45% w/w aq. solution) (1 mL) was added via a syringe. A white precipitate was formed instantaneously, which was re-dissolved over time. Addition of trimethylamine was repeated 5 times until there was no more formation of the precipitate. The crude polymer product was obtained by precipitating the reaction mixture in diethyl ether. After being collected by vacuum filtration and dried, the crude product was dissolved in methanol and re-precipitated in diethyl ether to produce an off-white powder.

### Synthesis of BPN

A mixture of 7-bromo-1,1,1-trifluoroheptane-2-one (0.88 g, 3.56 mmol), biphenyl (0.50 g, 3.24 mmol), dichloromethane (3.0 mL), and a stir bar were placed in a 20 mL glass vial cooled in an ice bath. Triflic acid (3.0 mL) was added in one portion, and the mixture was stirred for 30 min and slowly warmed to room temperature and stirred for an additional 3 h under nitrogen atmosphere. The resulting dark-brown, gel-like mass was then poured into warm methanol with stirring. White fibres were filtered and washed with methanol (BPBr). After drying under vacuum, 1.20 g of white fibre-like solid of BPBr was obtained. Trimethylamine aqueous solution (3.0 mL) was added to a solution of BPBr (1.2 g) in THF (5.0 mL) then stirred at room temperature. Deionized water (2 mL) was added to the solution to dissolve the formed precipitate. Volatiles were removed using a rotary evaporator, and the ionic polymer BPN was precipitated in diethyl ether, filtered, and dried under vacuum.

### Synthesis of TPN

TPBr was prepared using a similar procedure of BPBr from 7-bromo-1,1,1-trifluoroheptane-2-one (0.59 g, 2.39 mmol), m-terphenyl (0.50 g, 2.17 mmol), dichloromethane (3.0 mL), and triflic acid (3.0 mL). 0.98 g of white fibre-like solid was obtained. TPN was prepared using a similar procedure of BPN from TPBr. The thickness of wet TPN membranes is 30  $\mu\text{m}$ . The properties of the TPN membrane are reported elsewhere.<sup>32</sup>

### IEC measurement

IECs of the membranes were determined by Mohr titration. A piece of a fully dried membrane in chloride form was weighed out and then immersed in 0.5 M  $\text{NaNO}_3$  for at least 24 hrs. The  $\text{NaNO}_3$  solution was collected and titrated with 0.1 M  $\text{AgNO}_3$ , using a few drops of  $\text{K}_2\text{CrO}_4$  as a colorimetric indicator. The IEC value was obtained from the calculated mass of the membrane in hydroxide form and the amount  $\text{AgNO}_3$  consumed in the titration.

### Conductivity measurement

Each polymer membrane (approximate size of 3 cm  $\times$  0.5 cm) was converted to hydroxide form with 1M NaOH solution and washed thoroughly with fresh deionized water to remove residual hydroxide ions. The in-plane hydroxide conductivity ( $\sigma$  in  $\text{mS cm}^{-1}$ ) of each membrane (approximate size: 3 cm  $\times$  0.5 cm) was measured using a four-point probe electrode method with BT-512 membrane conductivity test system (BekkTech LLC). Measurements were carried out under fully hydrated conditions where the cell was fully immersed in deionized water which was degassed and blanketed with a flow of argon gas. The ionic conductivity was calculated according to

$$\sigma = L / (R \times W \times T)$$

where  $L$  is the distance between the two inner platinum wires (0.47 cm),  $R$  is the resistance of the membrane in ohms, and  $W$  and  $T$  are the width and the thickness of the membrane in centimetres, respectively.

### Water uptake measurement

The fully hydrated membrane in hydroxide form was taken out of the water and wiped quickly with filter paper. The weight of the wet membrane ( $W_{wet}$ ) was recorded. Then, membranes were dried at 80  $^\circ\text{C}$  overnight and the weight of the dry membrane ( $W_{dry}$ ) was determined. Water uptake (%) was calculated according to:

$$\text{Water uptake (\%)} = [(W_{wet} - W_{dry}) \times 100] / (W_{dry}).$$

### Alkaline-stability test

The alkaline-stability of the membranes was evaluated by comparing IEC value and hydroxide conductivity value of the pristine membrane with those of alkaline-exposed membranes. Alkaline-exposed membranes were obtained by fully immersing membranes in 1 M NaOH solution at 80  $^\circ\text{C}$  for

a designated time period. For the IEC measurement, the alkaline-exposed membranes were immersed in 1 M NaCl to exchange counter ion, before measuring the IEC value by Mohr titration and  $^1\text{H}$  NMR methods. For the hydroxide conductivity measurement, the membranes were treated with 1 M NaOH in inert gas condition and washed thoroughly with deionized water in order to remove residual ions on the surface of the membranes, before measuring hydroxide conductivity value at 80 °C.

### **Infrared studies**

*In-situ* Infrared Reflection Adsorption Spectroscopy (IRRAS) experiments were performed at room temperature using a Nicolet 8700 FT-IR spectrometer equipped with a Mercury Cadmium Telluride (MCT) detector cooled with liquid nitrogen. Details of the experimental setup has been described previously.<sup>16, 17</sup> For each spectrum, 32 interferograms were added together at a resolution of 4  $\text{cm}^{-1}$  with unpolarised light. Prior to any adsorption IR studies, a background spectrum was collected while holding the potential at 1.4 V. Absorbance units of the spectra are defined as  $A = -\log(R/R_0)$ , where R and  $R_0$  represent reflected IR intensities corresponding to the sample and reference single beam spectrum, respectively. Thus, a positive peak in the resulting spectrum indicates a production of species, while a negative peak indicates consumption or decrease in concentration of a species compared to the reference spectrum. The reference spectrum was collected on a clean Pt disc electrode while holding at 1.4 V vs. RHE for 30 sec. A ZnSe hemisphere was used as the IR window, and the working electrode was pressed against the window, creating a thin solution layer with a thickness of a few micrometres. The incident angle of the IR radiation passing through the ZnSe window was 36°. Nitrogen was used to purge the electrolyte while dry air was used to purge the spectrometer and chamber, reducing the spectral interference from ambient  $\text{CO}_2$ . For the adsorption studies, a thin film of ionomer was drop-casted onto a polycrystalline Pt disc electrode. The electrode was then immersed in a dilute electrolyte solution (0.05 M NaOH). IR spectra was collected while holding the potential at 0.1 V vs. RHE.

### **Microelectrode experiment**

FLN-55 and BPN ionomers in hydroxide form were dissolved in a water-isopropanol (20:80 v/v%) mixture to obtain 1 wt% solution. Later, 1 mg of Pt/C or RuPt/C catalysts added in the ionomer solution. The catalyst ink was sonicated for 1 hr. After sonication, a thin film was cast on the surface of the microelectrode from 2  $\mu\text{l}$  of the catalyst ink. The microelectrode was assembled to the Pt counter using an anion exchange membrane (benzyl trimethyl ammonium functionalized poly(phenylene) (ATM-PP)) as a conduction path between both electrodes and the reference electrode. The ATM-PP membrane was glued to the microelectrode and Pt counter electrode by FLN-55 or BPN ionomer. The assembled microelectrode was dried at 80 °C for 1 hr. The microelectrode was tested in a custom designed cell having the ATM-PP membrane in contact with a 0.1 NaOH solution and using a Hg/HgO electrode (XR400, Hach, Loveland, CO) as a reference electrode. The microelectrode was located at 1 cm of distance from the NaOH solution and exposed at 70% RH and 23 °C in the sealed cell.  $\text{N}_2$  was flowed to cure the microelectrode for 30 minutes prior to electrochemical stabilization. Then,  $\text{H}_2$  flowed to the cell for 30 minutes. Respective control characterization was performed under  $\text{N}_2$ .

### **Preparation of ionomer solution and MEA**

Both FLN and BPN ionomers in hydroxide form were soluble in methanol, dimethylsulfoxide, and *N*-dimethylformamide at room temperature but insoluble in water, acetone, and tetrahydrofuran. Therefore, the catalyst dispersions were prepared from the  $\text{OH}^-$  form of FLN and BPN ionomer dispersions in an alcoholic solvent mixture. FLN and BPN ionomers were converted to hydroxide form by immersing in 1 M NaOH solution for 24 h at room temperature followed by vigorous washing with deionized water and drying in the vacuum at 40 °C. The dried polymer was then dissolved in 1:1 v/v % ethanol-isopropanol to obtain 5 wt% solutions.

The catalyst ink was prepared using Pt/C (60 wt%, HISPEC® 9100, Johnson Matthey Fuel Cells, USA) and PtRu/C (Pt: 50 wt%, Ru: 25 wt%, HISPEC® 12100, Johnson Matthey Fuel Cells, USA) for cathode and anode, respectively. The catalyst and FLN or BPN ionomers were mixed in 20:80 v/v % water-isopropanol solution followed by sonication for 1 h. An I/C ratio (ionomer to catalyst) was kept at 42

vol% and 56.8 vol% for cathode and anode, respectively. Gas diffusion electrodes (GDEs) were prepared by hand painting catalyst inks onto gas diffusion layers (5 cm<sup>2</sup>, BC29, SGL Carbon) on the vacuum table at 60 °C. The Pt loading was 0.6 and 0.5 mg cm<sup>-2</sup> (and 0.25 mg<sub>Ru</sub> cm<sup>-2</sup>) in cathode and anode, respectively. The prepared electrodes and the TPN membrane were then immersed in 1 M NaOH solution to convert to hydroxide form. Further, the membrane was sandwiched between the electrodes and placed into the fuel cell hardware (area: 5 cm<sup>2</sup>, serpentine flow field, Fuel Cell Technologies, Inc., USA). No hot pressing was used; instead, the cell was assembled by applying 40 psi of torque.

For the Nafion-based MEA, the catalyst ink was prepared using Pt/C (60 wt%, HISPEC® 9100, Johnson Matthey Fuel Cells, USA) for both anode and cathode. The catalyst and commercial Nafion dispersion (Ion Power, DE521) were mixed by sonication for 1 h. The I/C ratio was kept at 42 vol% for cathode and anode. The GDEs were prepared using the BC29 gas diffusion layer as the same way for the AMFC MEAs. The Pt loading was 0.6 mg cm<sup>-2</sup> in cathode and anode. Nafion 211 (wet thickness: 30 μm) membrane was sandwiched between the electrodes and placed into the fuel cell hardware (area: 5 cm<sup>2</sup>, serpentine flow field, Fuel Cell Technologies, Inc., USA). No hot pressing was used; instead, the cell was assembled by applying 40 psi of torque.

### **Fuel cell test and performance evaluation**

Before testing the AMFC single cell, 5 ml of 1 M NaOH flowed into the fuel cell hardware followed by washing with 10 ml of deionized water. The cell temperature was raised to 80 °C before flowing the humidified gases. The H<sub>2</sub> and O<sub>2</sub> gases flowed into the cell at 100% RH. During the whole break-in process, the flow rates were kept at 2000 and 1000 sccm for hydrogen and oxygen, respectively. The polarization curves before break-in were obtained at various backpressures using a fuel cell station (Fuel Cell Technologies Inc., USA). Then, the cell was broke-in at a constant voltage of 0.5 V for 24 h. After break-in, the cell was cooled down to room temperature and replenished *in-situ* with 1 M NaOH as described earlier. Similarly, the temperature of the replenished cell was raised to 80 °C before flowing the humidified gases at 2000 sccm (H<sub>2</sub>) and 1000 sccm (O<sub>2</sub>). The current was measured at 0.5 V until it stabilizes. Before obtaining the first polarization curve, the pH of the anode and cathode effluents was checked to confirm that there is no residual NaOH. The polarization curves were recorded at different pressures and flow rate. The flow rates for H<sub>2</sub> and O<sub>2</sub> were 2000 (or 500) and 1000 (or 300) sccm, as specified. In-built Impedance analyser was used to measure the HFR while obtaining the polarization curves.

For the Nafion based MEA, cell break-in was performed at a constant voltage of 0.7 V at 80 °C overnight. During the break-in of the Nafion MEAs, the cell current increased and reached the plateau. The polarization curves were recorded after the break-in at 285 kPa. The flow rates for H<sub>2</sub> and O<sub>2</sub> were 300 and 500 sccm, respectively.

The extended-term test was performed at the constant current density of 0.6 A cm<sup>-2</sup>. The cell was operated at 80 °C, 147 kPa backpressure with flowing H<sub>2</sub> (2000 sccm) and O<sub>2</sub> (300 sccm) under fully humidified conditions. We stopped the cell operation at 200, 350, 480, and 550 h to obtain the polarization curves. Polarization curves were obtained after removing accumulated carbonated ions by the replenishing process described earlier. The polarization curves and the cell HFRs were obtained at 80 °C, 285 kPa backpressure with flowing H<sub>2</sub> (2000 sccm) and O<sub>2</sub> (300 sccm).

**Table S1.** IEC and hydroxide conductivity change during alkaline stability test (1 M NaOH at 80 °C)

Ionomer	IEC (meq. g <sup>-1</sup> )			$\sigma$ (mS cm <sup>-1</sup> ) <sup>a</sup>	
	Initial	240 h	500 h	Initial	500 h
<b>FLN-30</b>	1.50 ± 0.03	1.58 ± 0.03	1.55 ± 0.03	105 ± 5	103 ± 5
<b>FLN-40</b>	2.10 ± 0.03	2.15 ± 0.03	2.14 ± 0.03	119 ± 5	126 ± 5
<b>FLN-55</b>	2.48 ± 0.04	2.53 ± 0.04	2.42 ± 0.04	120 ± 7	NA <sup>b</sup>

<sup>a</sup> measured at 80 °C,<sup>b</sup> NA: not available

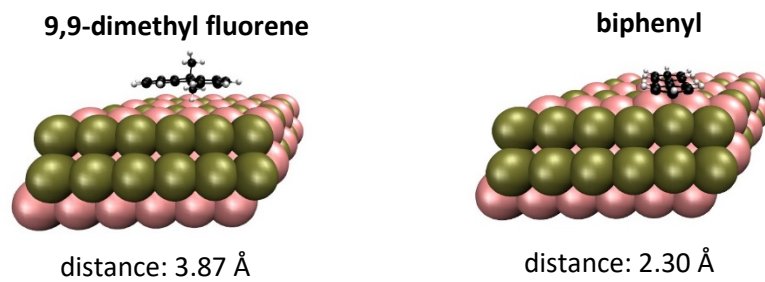


**Figure S1.** Average orthogonal distance between the carbon atoms of the 9,9-dimethyl fluorene and biphenyl and PtRu metal surface.

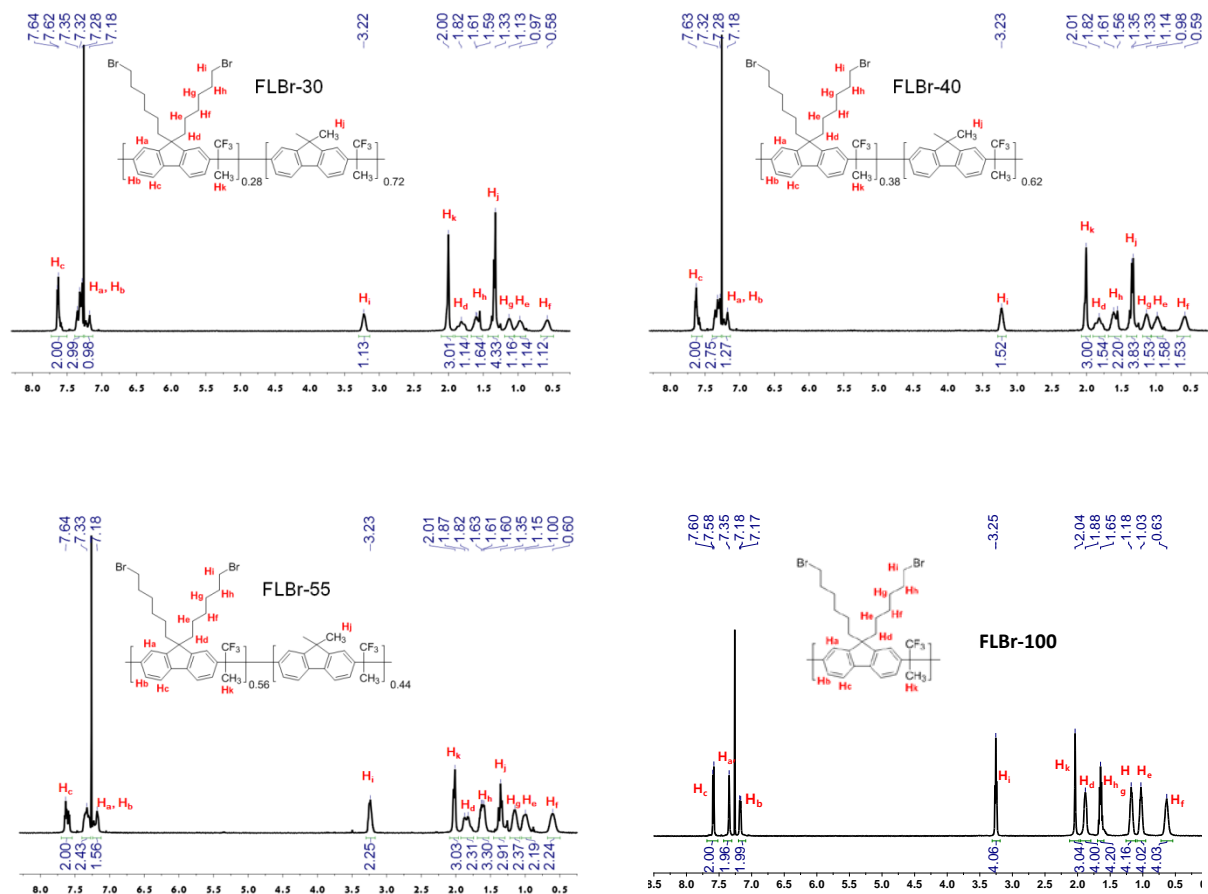


**Figure S2.** <sup>1</sup>H NMR spectra of FLBr-xx (xx = 30, 40, 55 and 100).

**FLBr-30** <sup>1</sup>H NMR (500 MHz, CDCl<sub>3</sub>): 7.62 (2H, Ar H), 7.18-7.36 (4H, Ar H), 3.22 (1.12H; CH<sub>2</sub>Br), 2.00 (3H, CF<sub>3</sub>CCH<sub>3</sub>); 1.82 (1.12H, CH<sub>2</sub>), 1.61 (1.12H, CH<sub>2</sub>), 1.33 (4.32H, CH<sub>3</sub>CCH<sub>3</sub>), 1.13 (1.12H, CH<sub>2</sub>), 0.97 (1.12H, CH<sub>2</sub>), 0.58 (1.12H, CH<sub>2</sub>).

**FLBr-40** <sup>1</sup>H NMR (500 MHz, CDCl<sub>3</sub>): 7.63(2H, Ar H), 7.18-7.36 (4H, Ar H), 3.22 (1.52H; CH<sub>2</sub>Br), 2.01 (3H, CF<sub>3</sub>CCH<sub>3</sub>); 1.82 (1.52H, CH<sub>2</sub>), 1.58 (1.52H, CH<sub>2</sub>), 1.33 (3.72H, CH<sub>3</sub>CCH<sub>3</sub>), 1.14 (1.52H, CH<sub>2</sub>), 0.98 (1.52H, CH<sub>2</sub>), 0.59 (1.52H, CH<sub>2</sub>).

**FLBr-55** <sup>1</sup>H NMR (500 MHz, CDCl<sub>3</sub>): 7.63(2H, Ar H), 7.18-7.36 (4H, Ar H), 3.23 (2.24H; CH<sub>2</sub>Br), 2.01 (3H, CF<sub>3</sub>CCH<sub>3</sub>); 1.82 (2.24H, CH<sub>2</sub>), 1.58 (2.24H, CH<sub>2</sub>), 1.35 (2.64H, CH<sub>3</sub>CCH<sub>3</sub>), 1.14 (2.24H, CH<sub>2</sub>), 0.99 (2.24H, CH<sub>2</sub>), 0.61 (2.24H, CH<sub>2</sub>).

**FLBr-100** <sup>1</sup>H NMR (500 MHz, CDCl<sub>3</sub>): 7.60 (2H, Ar H), 7.35 (2H, Ar H), 7.18 (2H, Ar H), 3.25 (4H; CH<sub>2</sub>Br), 2.04 (3H, CF<sub>3</sub>CCH<sub>3</sub>); 1.88 (4H, CH<sub>2</sub>), 1.65 (4H, CH<sub>2</sub>), 1.18 (4H, CH<sub>2</sub>), 1.03 (4H, CH<sub>2</sub>), 0.63 (4H, CH<sub>2</sub>).

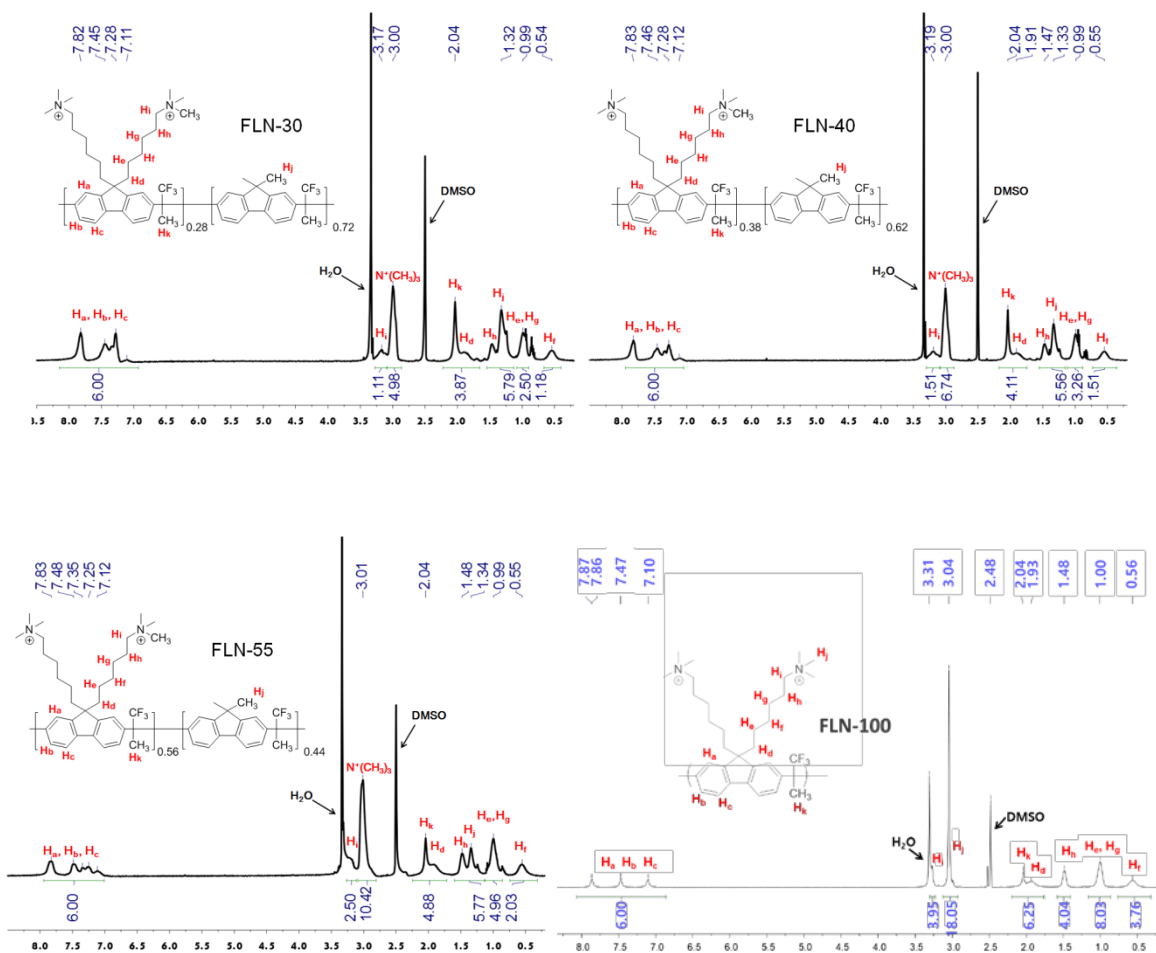


**Figure S3.**  $^1\text{H}$  NMR spectra of FLN-xx (xx = 30, 40, 55, and 100).

**FLN-30**  $^1\text{H}$  NMR (500 MHz,  $\text{DMSO-}d_6$ ): 7.12-7.83 (6H, Ar H), 3.19 (1.12H;  $\text{CH}_2\text{N}$ ), 3.00 (5.04H,  $\text{CH}_3\text{N}$ ), 2.04 (3H,  $\text{CF}_3\text{CCH}_3$ ), 1.91 (1.12H,  $\text{CH}_2$ ), 1.47 (1.12H,  $\text{CH}_2$ ), 1.33 (4.32H,  $\text{CH}_3\text{CCH}_3$ ), 0.99 (1.12H,  $\text{CH}_2$ ), 0.55 (1.12H,  $\text{CH}_2$ ).

**FLN-40**  $^1\text{H}$  NMR (500 MHz,  $\text{DMSO-}d_6$ ): 7.12-7.83 (6H, Ar H), 3.19 (1.52H;  $\text{CH}_2\text{N}$ ), 3.00 (6.84H,  $\text{CH}_3\text{N}$ ), 2.04 (3H,  $\text{CF}_3\text{CCH}_3$ ), 1.91 (1.52H,  $\text{CH}_2$ ), 1.47 (1.52H,  $\text{CH}_2$ ), 1.33 (3.72H,  $\text{CH}_3\text{CCH}_3$ ), 0.99 (1.52H,  $\text{CH}_2$ ), 0.55 (1.52H,  $\text{CH}_2$ ).

**FLN-55**  $^1\text{H}$  NMR (500 MHz,  $\text{DMSO-}d_6$ ): 7.12-7.83 (6H, Ar H), 3.19 (2.24H;  $\text{CH}_2\text{N}$ ), 3.00 (10.08H,  $\text{CH}_3\text{N}$ ), 2.04 (3H,  $\text{CF}_3\text{CCH}_3$ ), 1.91 (2.24H,  $\text{CH}_2$ ), 1.47 (2.24H,  $\text{CH}_2$ ), 1.33 (2.64H,  $\text{CH}_3\text{CCH}_3$ ), 0.99 (2.24H,  $\text{CH}_2$ ), 0.55 (2.24H,  $\text{CH}_2$ ).

**FLN-100**  $^1\text{H}$  NMR (500 MHz,  $\text{DMSO-}d_6$ ): 7.12-7.83 (6H, Ar H), 3.31 (4H;  $\text{CH}_2\text{N}$ ), 3.00 (18H,  $\text{CH}_3\text{N}$ ), 2.04 (3H,  $\text{CF}_3\text{CCH}_3$ ), 1.91 (4H,  $\text{CH}_2$ ), 1.47 (4H,  $\text{CH}_2$ ), 0.99 (8H,  $\text{CH}_2$ ), 0.55 (4H,  $\text{CH}_2$ ).

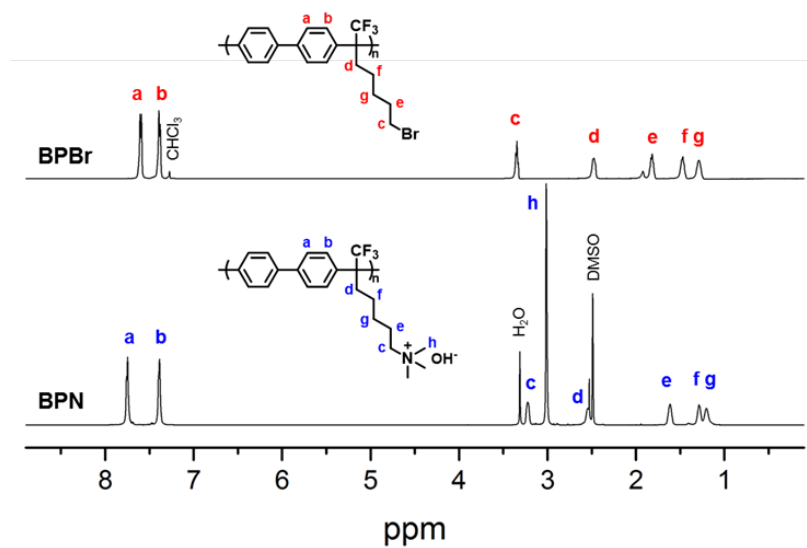


**Figure S4.** <sup>1</sup>H NMR spectra of BPBr and BPN (in CDCl<sub>3</sub> and DMSO-d<sub>6</sub>, respectively).

**BPBr.** <sup>1</sup>H NMR (500 MHz, CDCl<sub>3</sub>): 7.56 (4H, Ar H), 7.35 (4H, Ar H), 3.32 (2H, CH<sub>2</sub>Br), 2.43 (2H, CF<sub>3</sub>CCH<sub>2</sub>), 1.78 (2H, CH<sub>2</sub>), 1.43 (2H, CH<sub>2</sub>), 1.24 (2H, CH<sub>2</sub>).

**BPN.** <sup>1</sup>H NMR (500 MHz, DMSO-d<sub>6</sub>): 7.75 (4H, Ar H), 7.39 (4H, Ar H), 3.21 (2H, CH<sub>2</sub>N(CH<sub>3</sub>)<sub>3</sub>), 3.02 (9H, N(CH<sub>3</sub>)<sub>3</sub>), 2.54 (2H, CH<sub>2</sub>), 1.61 (2H, CH<sub>2</sub>), 1.28 (2H, CH<sub>2</sub>), 1.21 (2H, CH<sub>2</sub>).

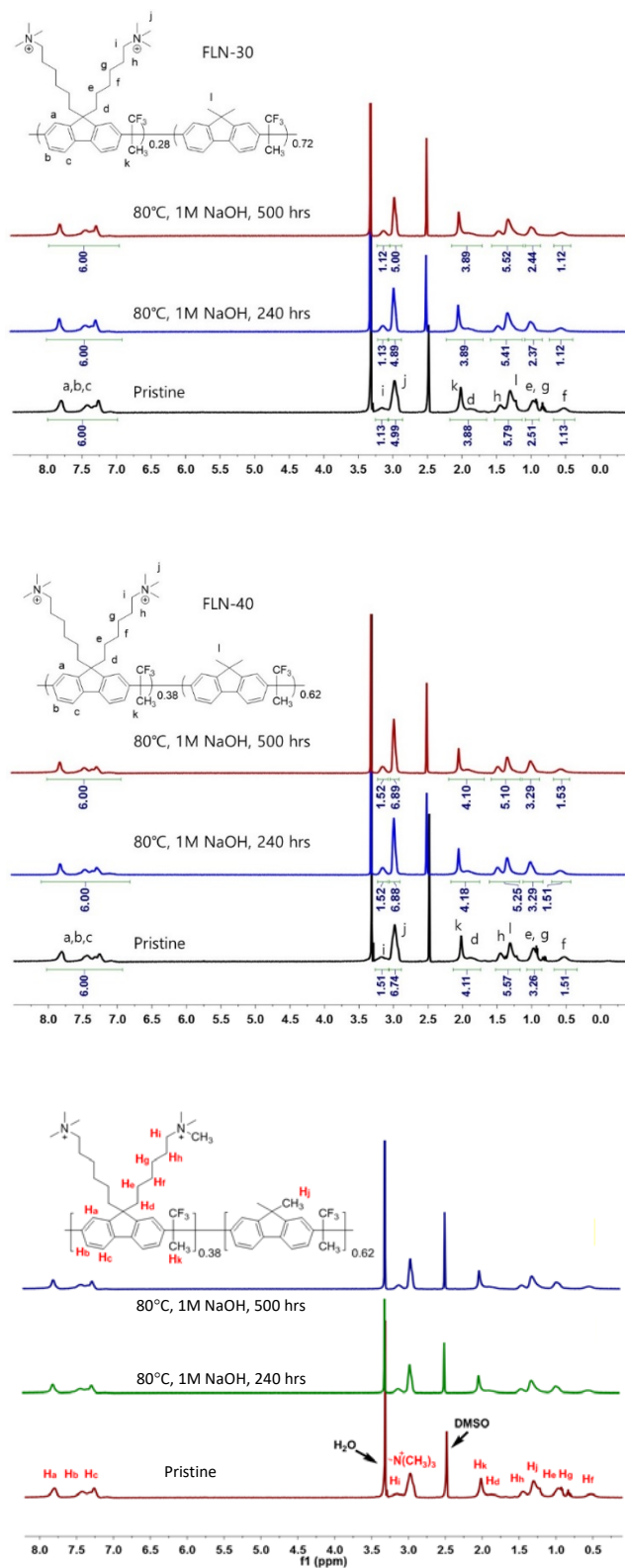


**Figure S5.**  $^1\text{H}$  NMR spectra of FLN-30, FLN-40 and FLN-55 before and after alkaline stability test in 1 M NaOH at 80 °C.

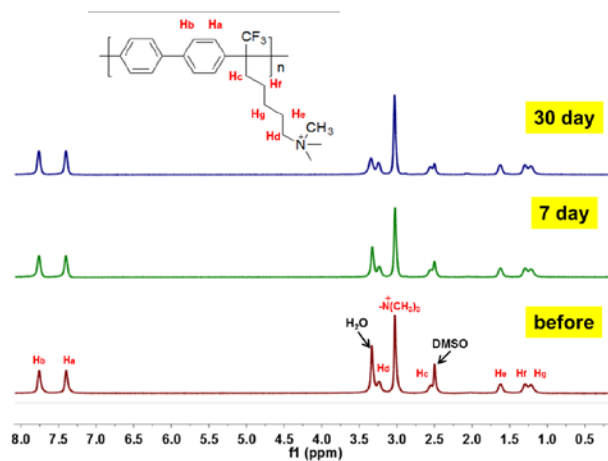


**Figure S6.** <sup>1</sup>H NMR spectra of BPN before and after alkaline stability test in 1 M NaOH at 80 °C.

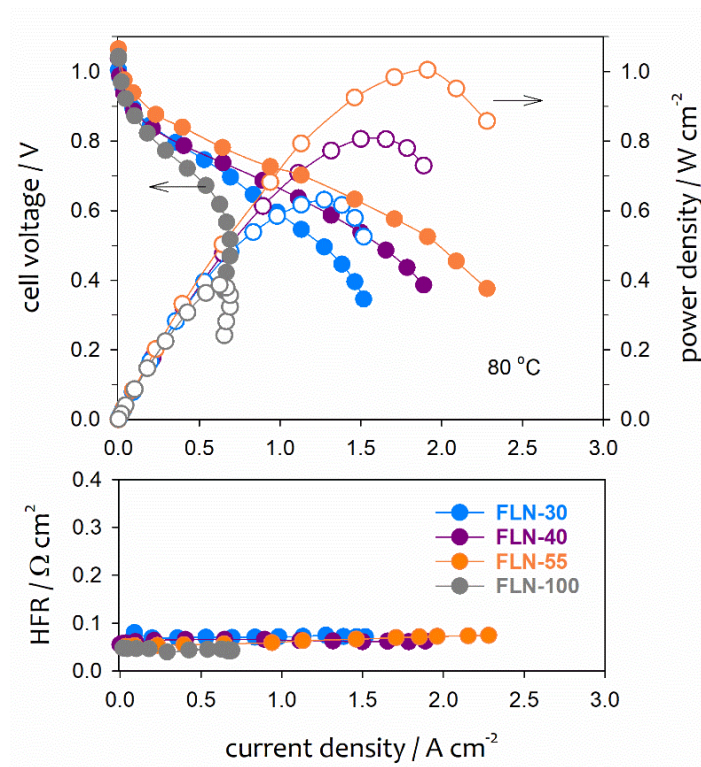


**Figure S7.** Impact of ionomer IEC on AMFC performance operating at 80 °C with fully humidified H<sub>2</sub> (500 sccm) and O<sub>2</sub> (300 sccm) at 285 kPa backpressure. Anode: Pt-Ru/C (0.5 mg<sub>Pt</sub> cm<sup>-2</sup>), cathode: Pt/C (0.6 mg<sub>Pt</sub> cm<sup>-2</sup>).

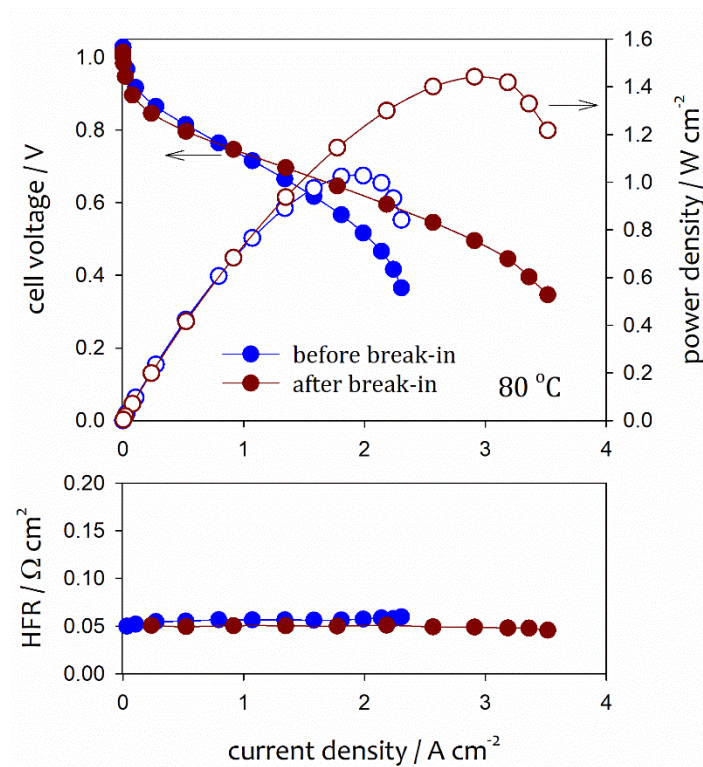


**Figure S8.** Comparison of pre- and post-break-in AMFC performance of a MEA employing the FLN-55 ionomer operating at  $80\text{ }^{\circ}\text{C}$  with fully humidified  $\text{H}_2$  (2000 sccm) and  $\text{O}_2$  (1000 sccm) at 285 kPa backpressure. Anode: Pt-Ru/C ( $0.5\text{ mg}_{\text{Pt}}\text{ cm}^{-2}$ ), cathode: Pt/C ( $0.6\text{ mg}_{\text{Pt}}\text{ cm}^{-2}$ ).

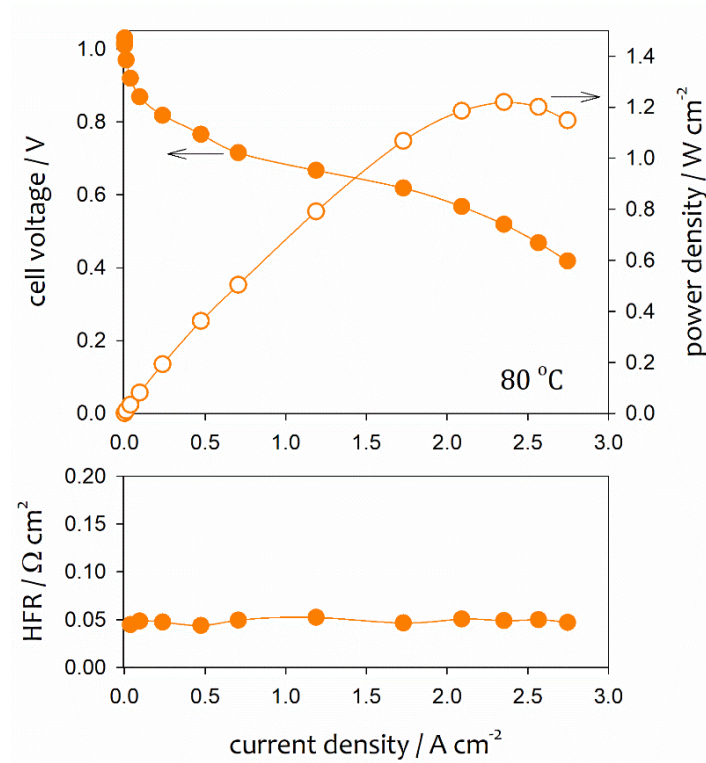


**Figure S9.** AMFC performance of BPN ionomer at 80 °C with fully humidified H<sub>2</sub> (2000 sccm) and O<sub>2</sub> (1000 sccm) at 285 kPa backpressure. Anode: Pt-Ru/C (0.5 mg<sub>Pt</sub> cm<sup>-2</sup>), cathode: Pt/C (0.6 mg<sub>Pt</sub> cm<sup>-2</sup>).

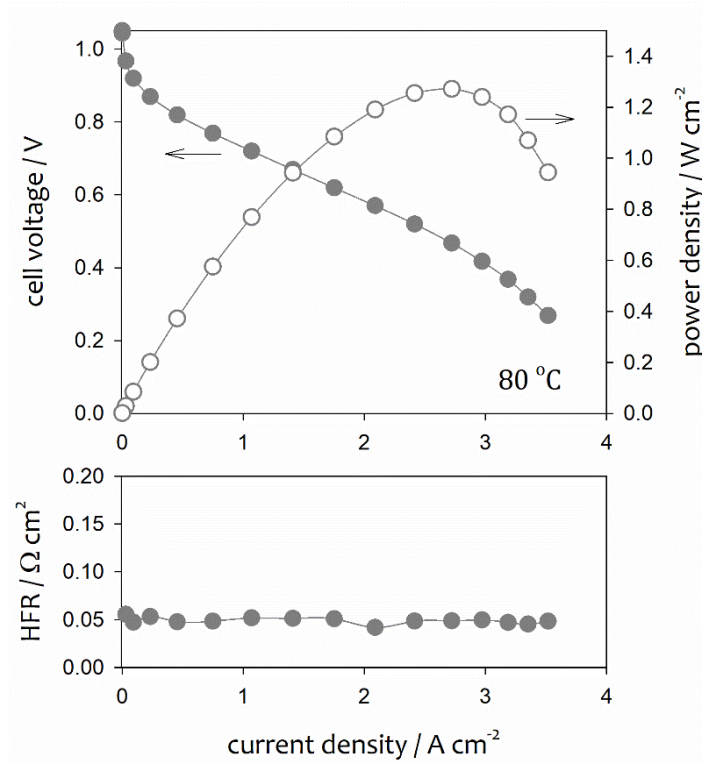


**Figure S10.** AMFC performance of FLN-55 ionomer at 80 °C with fully humidified  $\text{H}_2$  (2000 sccm) and  $\text{O}_2$  (1000 sccm) at 285 kPa backpressure. Anode and cathode: Pt/C ( $0.6 \text{ mg}_{\text{Pt}} \text{ cm}^{-2}$ ).

## References

1. M. Dion, H. Rydberg, E. Schroder, D. C. Langreth and B. I. Lundqvist, *Phys. Rev. Lett.*, 2004, **92**, 246401.
2. G. Roman-Perez and J. M. Soler, *Phys. Rev. Lett.*, 2009, **103**, 096102.
3. J. Klimes, D. R. Bowler and A. Michaelides, *Phys. Rev. B*, 2011, **83**, 195131.
4. P. E. Blochl, *Phys. Rev. B*, 1994, **50**, 17953-17979.
5. G. Kresse and D. Joubert, *Phys. Rev. B*, 1999, **59**, 1758-1775.
6. G. Kresse and J. Hafner, *Phys. Rev. B*, 1993, **47**, 558-561.
7. G. Kresse and J. Hafner, *Phys. Rev. B*, 1994, **49**, 14251-14269.
8. G. Kresse and J. Furthmuller, *Comp. Mater. Sci.*, 1996, **6**, 15-50.
9. G. Kresse and J. Furthmuller, *Phys. Rev. B*, 1996, **54**, 11169-11186.
10. H. J. Monkhorst and J. D. Pack, *Phys. Rev. B*, 1976, **13**, 5188-5192.
11. M. Methfessel and A. T. Paxton, *Phys. Rev. B*, 1989, **40**, 3616-3621.
12. M. K. Sabbe, L. Lain, M. F. Reyniers and G. B. Marin, *Phys. Chem. Chem. Phys.*, 2013, **15**, 12197-12214.
13. M. Saeys, M. F. Reyniers, G. B. Marin and M. Neurock, *J. Phys. Chem. B*, 2002, **106**, 7489-7498.
14. B. Muthuraj, S. Mukherjee, C. R. Patra and P. K. Iyer, *ACS Appl. Mater. Interfaces*, 2016, **8**, 32220-32229.
15. G. Saikia and P. K. Iyer, *J. Org. Chem.*, 2010, **75**, 2714-2717.
16. H. T. Chung, U. Martinez, J. Chlistunoff, I. Matanovic and Y. S. Kim, *J. Phys. Chem. Lett.*, 2016, **7**, 4464-4469.
17. S.-D. Yim, H. T. Chung, J. Chlistunoff, D.-S. Kim, C. Fujimoto, T.-H. Yang and Y. S. Kim, *J. Electrochem. Soc.*, 2015, **162**, F499-F506.